

Molybdenum Disulfide (MoS₂) along with Graphene Nanoplatelets (GNPs) Utilized to Enhance the Capacitance of Conducting Polymers (PANI and PPy)

Saima Nawaz^{a,b}, Yaqoob Khan^b, Sadia Khalid^b, Muhammad Azad Malik^{c*}, and M. Siddiq^{a*}

a. Department of Chemistry, Quaid-i-Azam University, Islamabad 45320, Pakistan.

b. Nanoscience and Technology Department, National Centre for Physics, QAU Campus, Shahdra Valley Road, Islamabad 45320, Pakistan.

c. Department of Chemistry, University of Zululand, Private bag X1001 KwaDlangezwa, 3880, South Africa.

*Address correspondence to:

Email address: m_sidiq12@yahoo.com

Tel.: +92 5190642147

Email: malikmohammad187@gmail.com

Tel.: +44 7403781143

Material Characterization of Mo(dtc)₄

Synthesized *Tetrakis*(diethyldithiocarbamato) molybdenum (IV) *i.e.* Mo(dtc)₄ was characterized by elemental analysis, FT-IR and thermogravimetric analyses as discussed below.

Elemental Analysis

The theoretical values calculated (*i.e.* Anal. Calc.) for Mo(dtc)₄; C₂₀H₄₀N₄S₈Mo are C, 34.9; H 5.9; N, 8.1%^{1,2} and in our synthesized Mo(dtc)₄ the values found are C, 34.9; H, 5.9; N, 8.1% using an organic elemental analyzer of Thermo Scientific Flash 2000.

Fourier Transform Infrared Spectroscopy (FT-IR)

FT-IR spectrum of Mo(dtc)₄ (Figure S1) is showing the peaks/bands at 2971, 2933, 2869, 1516, 1491, 1455, 1428, 1376, 1352, 1269, 1210, 1145, 1095, 1074, 1003 and 990 cm⁻¹ which are consistent with earlier reports¹⁻³. Three basic regions exist in infrared spectra of dithiocarbamato complexes;

- The first main region extends from 1450 to 1550 cm⁻¹ and account for thioureide (NCSS) band which typically occurs betwixt C-N and C=N band. The absorption band at 1500 cm⁻¹ is attributed as arising from polar structure —NCS₂.
- The second region (1070-930 cm⁻¹) is descriptive of mode of coordination in dithiocarbamato moiety (CSS).
- The third region around 350-400 cm⁻¹ is attributed to M-S bonds.¹⁻³

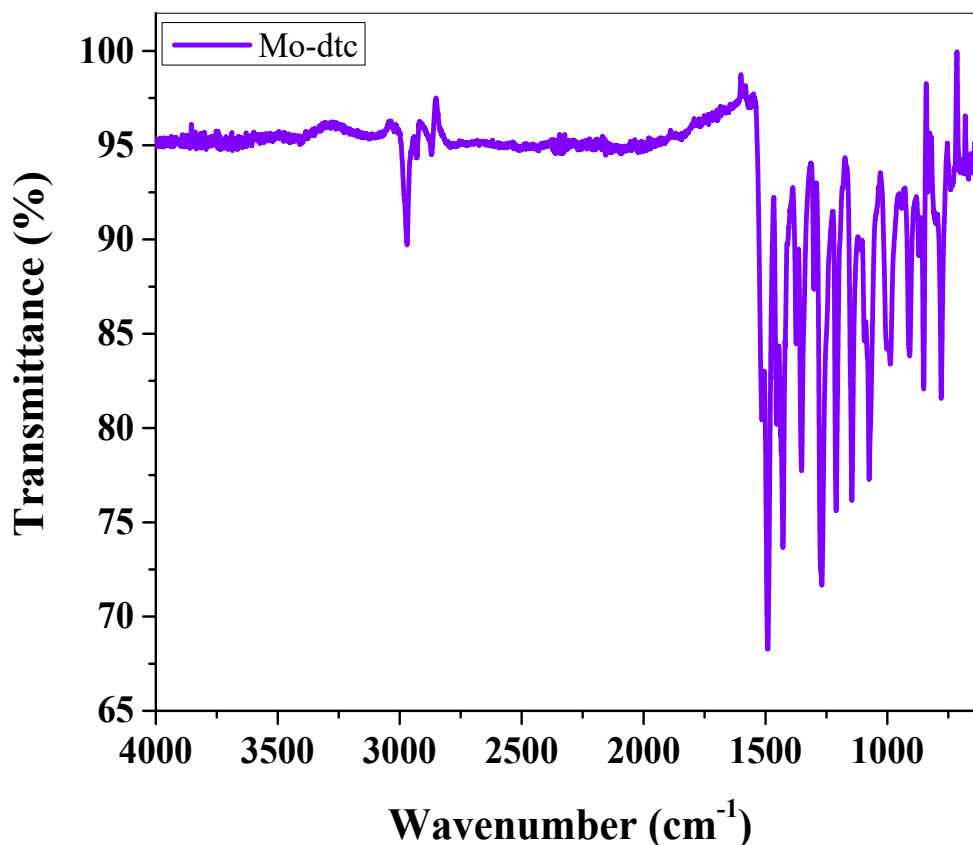


Figure S1: Fourier transform infrared (FT-IR) spectroscopy of Mo(dtc)₄.

Thermogravimetric Analysis (TGA)

Figure S2 displays the TGA of Mo(dtc)₄ under the environment of nitrogen. Three stages of decomposition take place at 151, 233, and 352 °C. The first -7.2 % decomposition step at 151 °C is due to the loss of ethylene (-4.0% calculated weight% loss) while -41.8% second step at 233 °C is due to two diethyldithiocarbamate molecules (-42.9% calculated weight% loss). The remaining material is a black solid with a residual weight percent of 28.3% after the third decomposition process (-22.7%). This thermal decomposition of Mo(dtc)₄ consequences to produce (23.5% calculated weight%) pure MoS₂, while additional 4.8% is due to decomposed ligand contamination.⁴

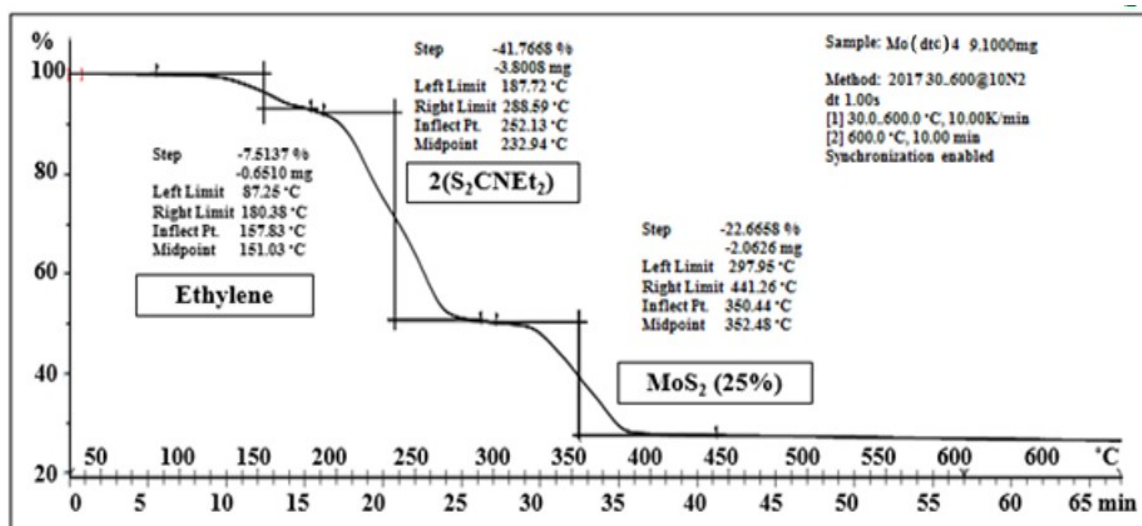


Figure S2: Thermogravimetric analysis (TGA) of Mo(dtc)₄.

Raman Analysis of MoS₂ melt

Raman spectra (Figure S3) indicates that thermolysis process under argon inert environment yields MoS₂ with A_{1g} out-of-plane mode centered at 361 cm⁻¹ and E_{12g} in-plane mode seen at 334 cm⁻¹ ($\Delta\nu = 27$ cm⁻¹).⁵ Phonon confinement may be the reason for softening of two modes and peaks broadening, which depicted that achieved resultant MoS₂ material is of few layers.^{6,7}

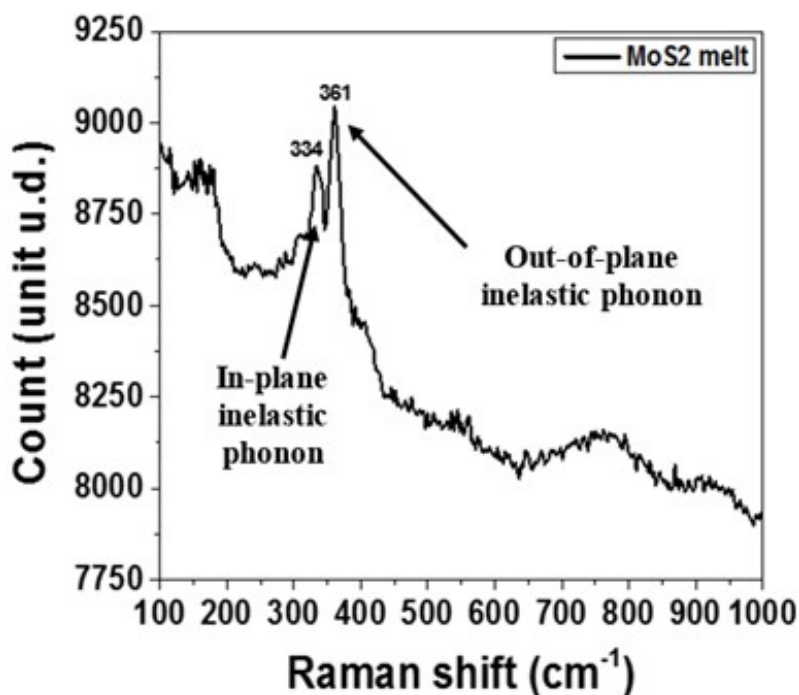


Figure S3: Raman analysis of MoS₂ melt.

Electrochemical Studies

Cyclic Voltammetry (CV)

CV at Various Scan Rates

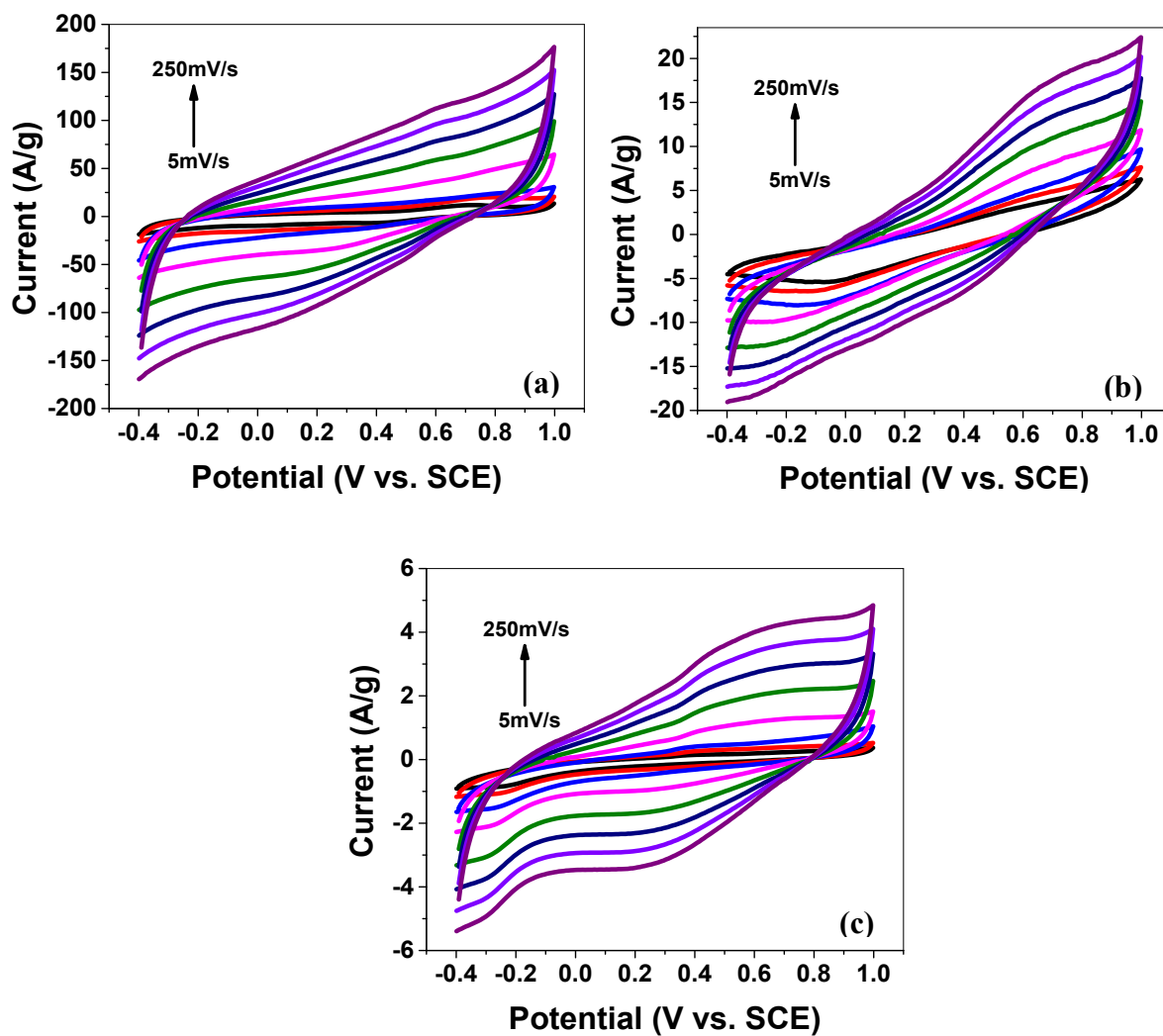


Figure S4: Cyclic voltammetry (CV) of (a) M5, (b) mPP and (c) mP at different scan rates on GCE in 1M H₂SO₄ vs. SCE.

Cyclic Stability for 50 Cycles of CV

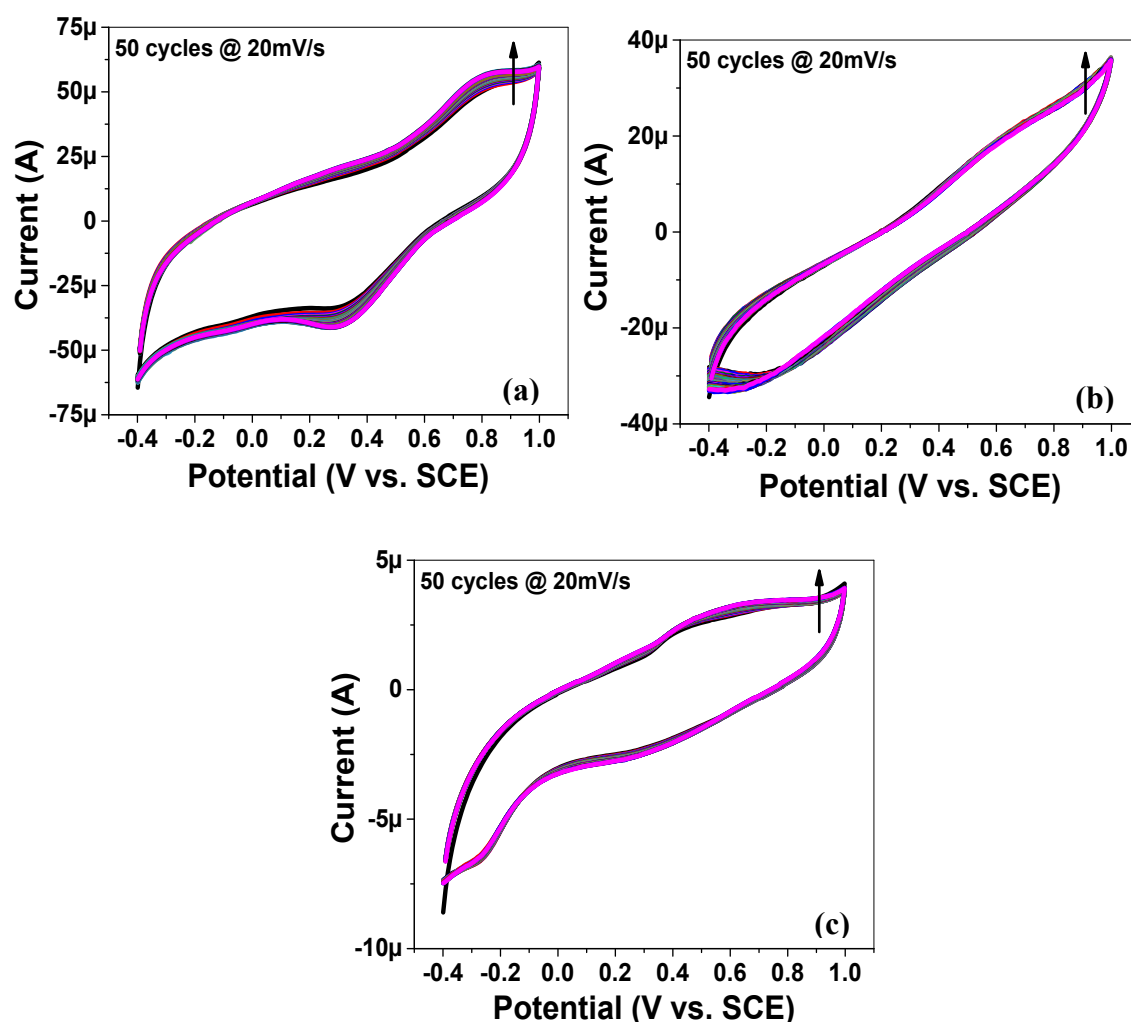


Figure S5: Cyclic voltammetry (CV): cyclic stability of (a) M5, (b) mPP and (c) mP at scan rate of 20mV/s for 50 cycles on GCE in 1M H₂SO₄ electrolyte vs. SCE.

EIS (Electrochemical Impedance Spectroscopy)

EIS Nyquist plots

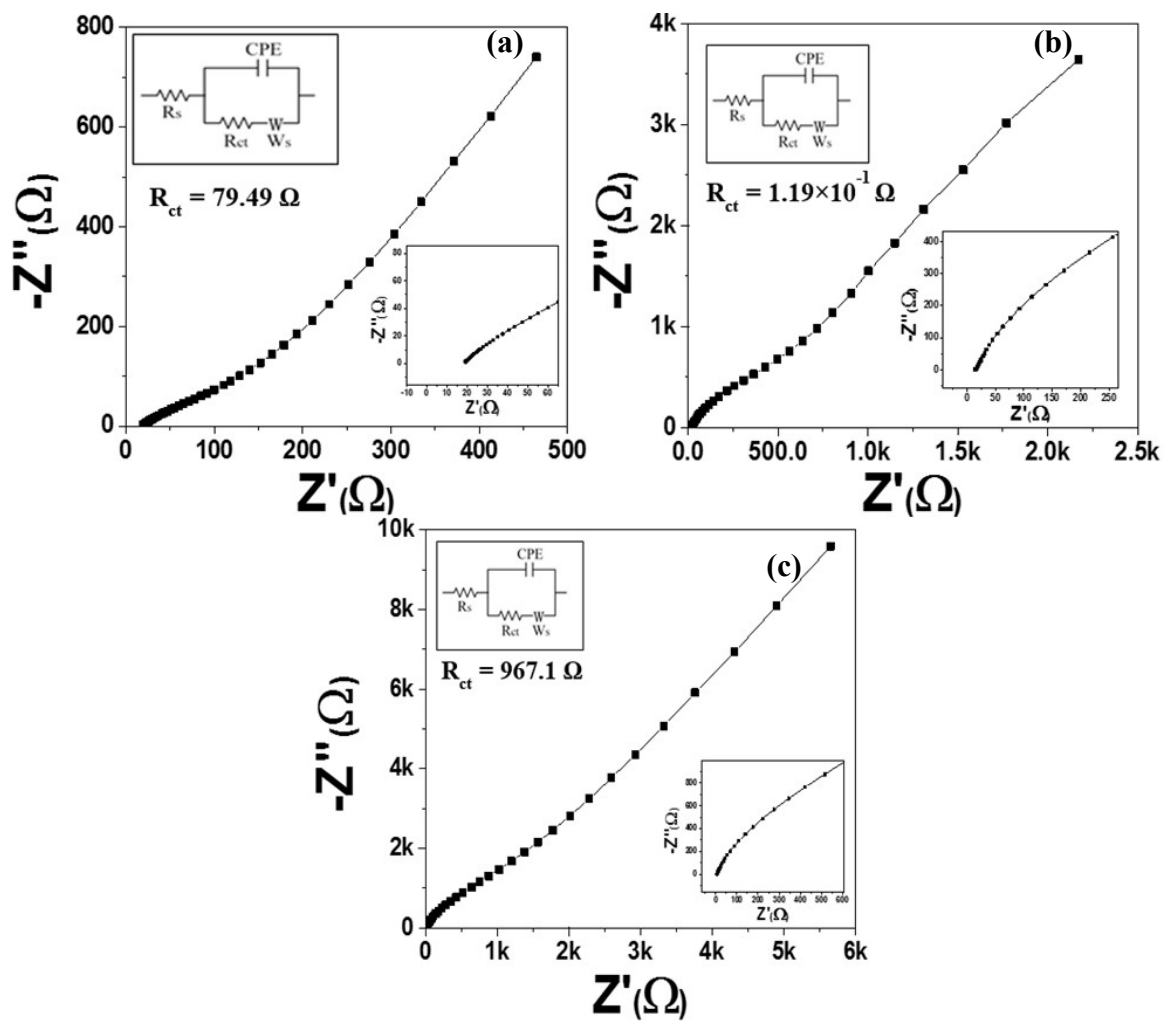


Figure S6: EIS Nyquist plots of (a) M5, (b) mPP and (c) mP vs. OC in 1M H_2SO_4 electrolyte with equivalent circuit diagram.

EIS Bode plots

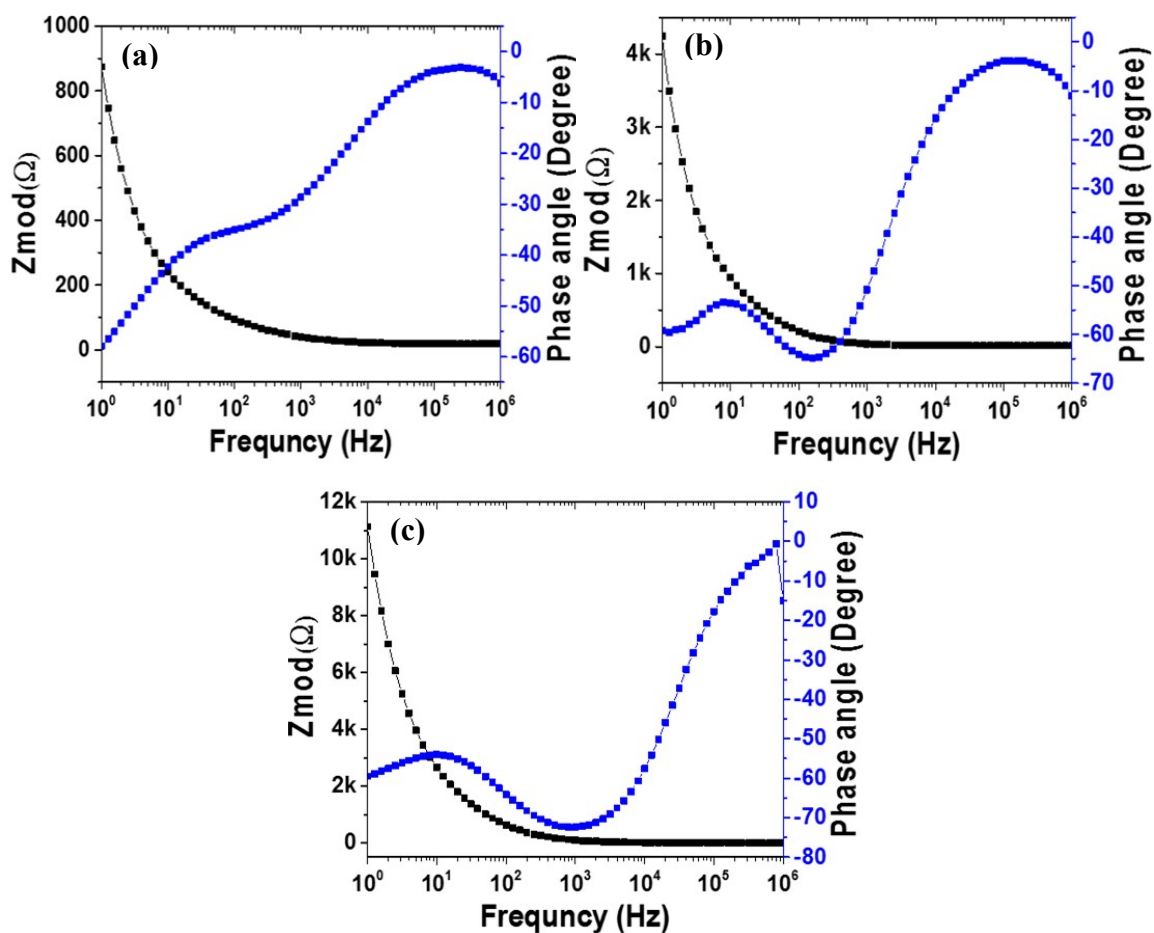


Figure S7: EIS (Electrochemical Impedance Spectroscopy): Bode plots of (a) M5, (b) mPP and (c) mP vs. OC (open circuit) at 10mv rms AC perturbation (in 1M H_2SO_4 electrolyte).

Galvanostatic Charge/Discharge (GCCD) Measurements

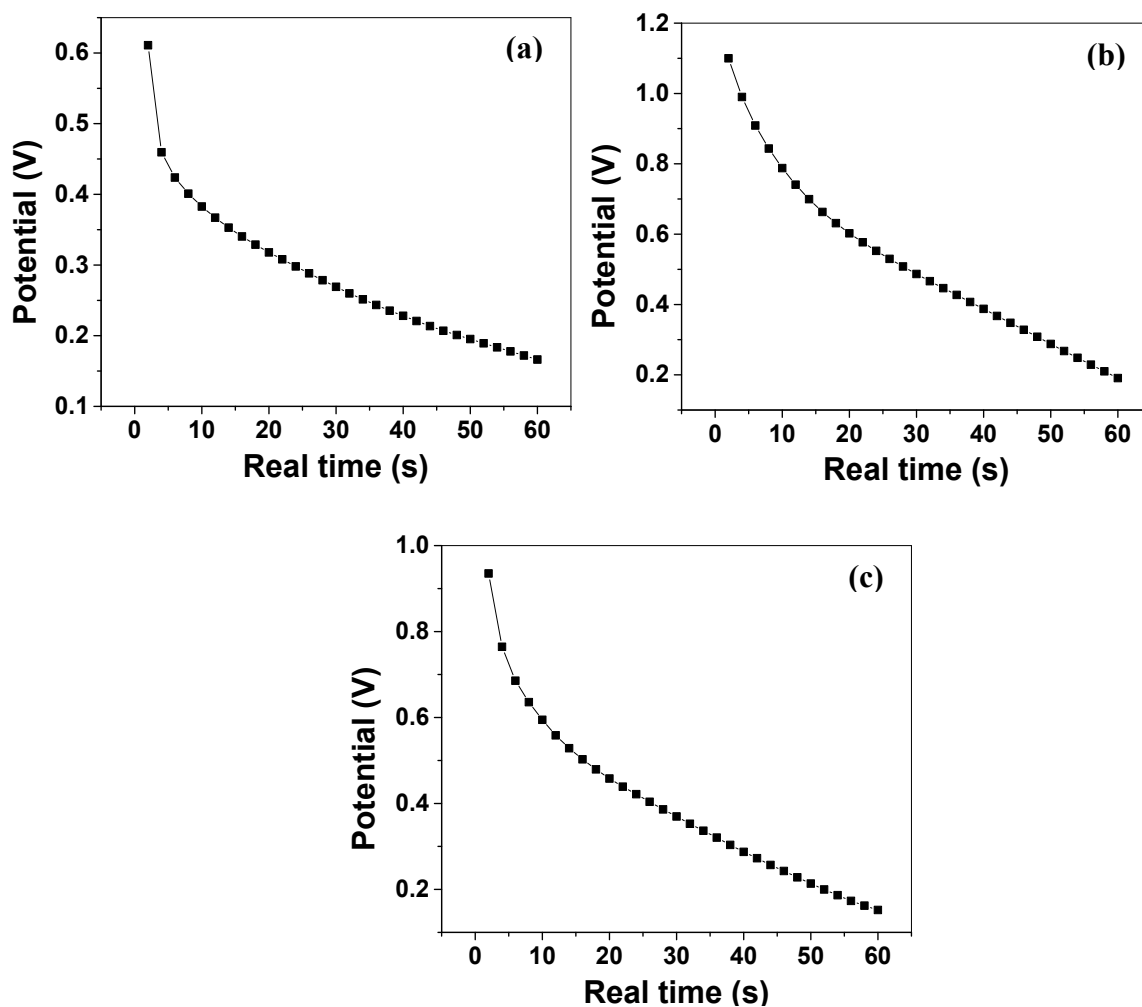


Figure S8: GCCD (Galvanostatic cyclic charge discharge): Discharge curve of (a) M5, (b) mPP and (c) mP Potential vs. real time (at charge density= 0.57 A/g) in 1M H₂SO₄ electrolyte.

Galvanostatic Charge/Discharge (GCCD) Measurements at different charge densities

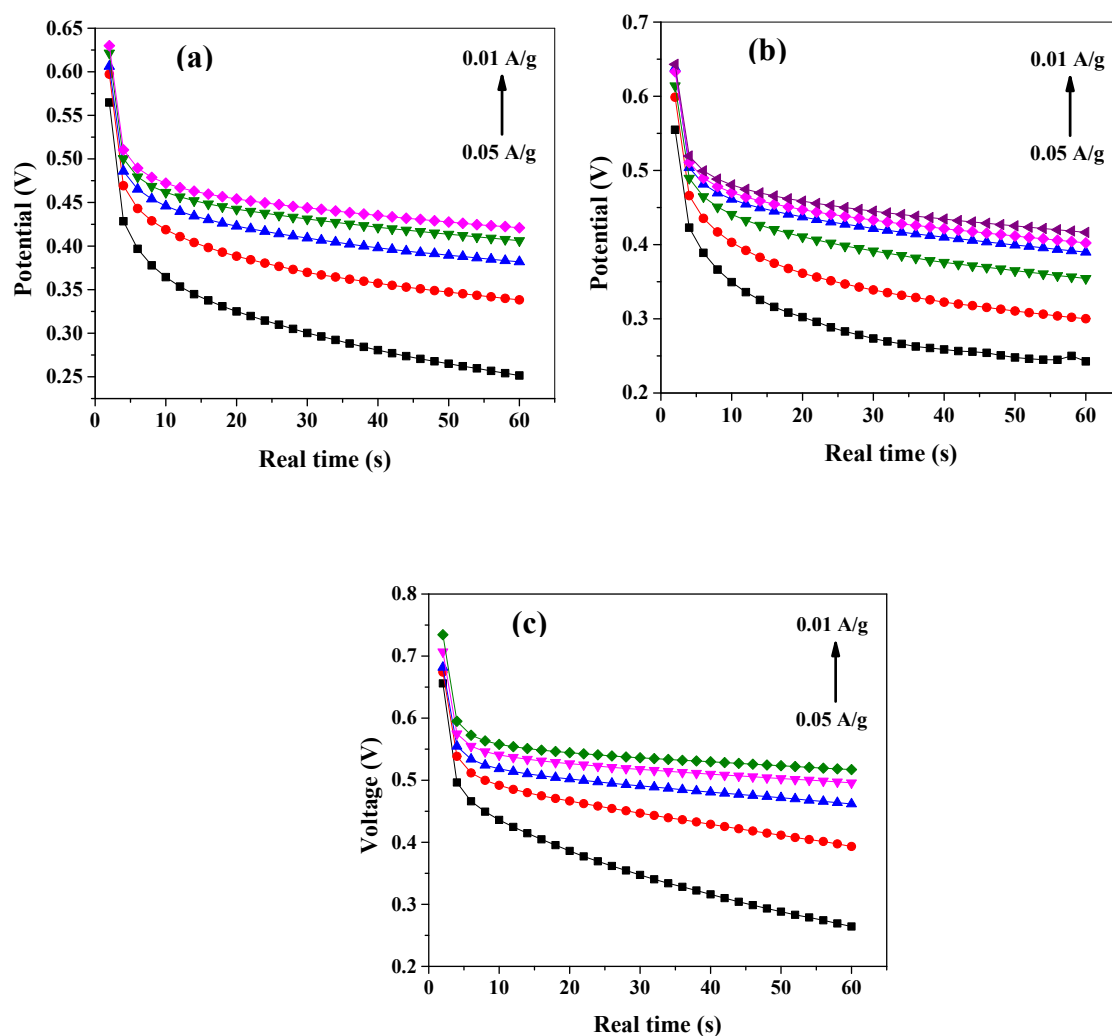


Figure S9: GCCD (Galvanostatic cyclic charge discharge): Discharge curve of (a) MoS₂ melt 5mPP, (b) MoS₂ melt 5mP and (c) MoS₂ melt Potential vs. real time at different charge densities in 1M H₂SO₄ electrolyte.

Galvanostatic Charge/Discharge (GCCD) Capacitance retention of MoS₂ melt 5mPP vs. cycle number for 10,000 cycles

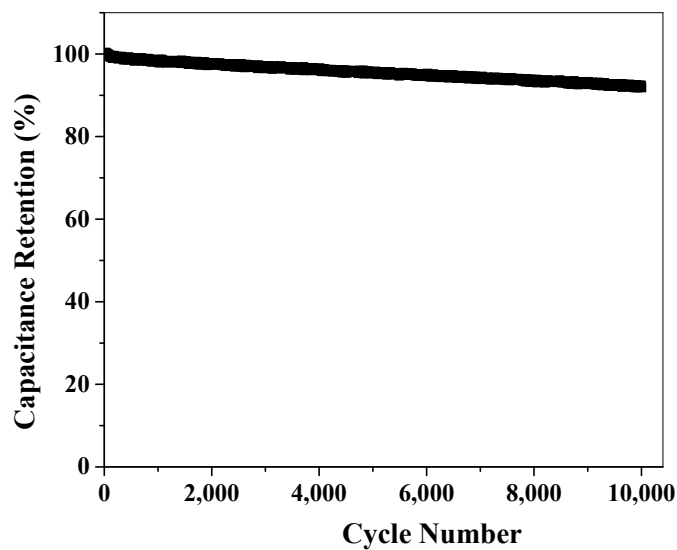


Figure S10: GCCD: Capacitance retention of MoS₂ melt 5mPP vs. cycle number for 10,000 cycles (in 1M H₂SO₄ electrolyte).

Capacitance retention of MoS₂ melt 5mPP for 10,000 charge-discharge cycles in 1M H₂SO₄ electrolyte is shown in Figure S10. The composite demonstrates improved charge storage performance and excellent cyclic stability (91.87% capacitance retention at 0.57 A/g after 10,000 cycles).

Raman Analysis of M5-Graphene nanoplatelets

Raman spectra for M5-Graphene nanoplatelets is shown in Figure S11.

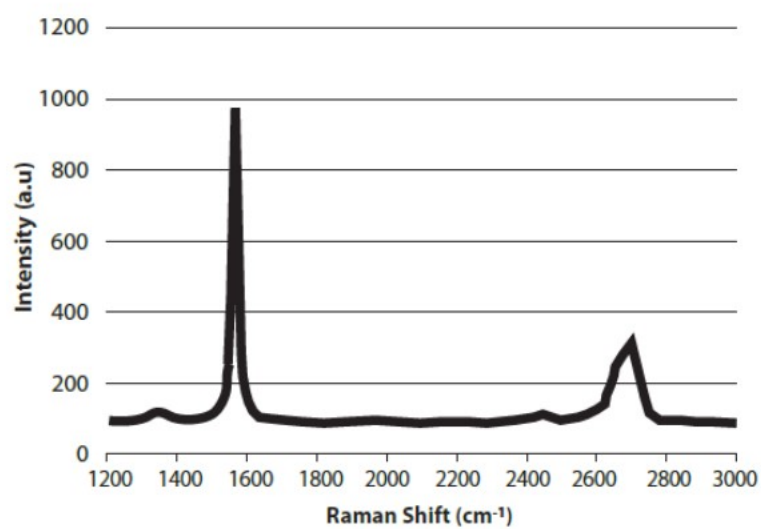


Figure S11: Raman analysis of M5.

Notes and References

1. D. J. Lewis, A. A. Tedstone, X. L. Zhong, E. A. Lewis, A. Rooney, N. Savjani, J. R. Brent, S. J. Haigh, M. G. Burke, C. A. Muryn, J. M. Raftery, C. Warrens, K. West, S. Gaemers, and P. O'Brien, *Chemistry of Materials*, 2015, 27, 1367-1374.
2. E. P. C. Higgins, S. G. McAdams, D. G. Hopkinson, C. Byrne, A. S. Walton, D. J. Lewis, and R. A. W. Dryfe, *Chemistry of Materials*, 2019, 31, 5384-5391.
3. A. Nieuwpoort, *Dithiolato complexes of molybdenum and tungsten*, 1975, Katholieke Universiteit Nijmegen (Netherlands).
4. M. N. McCain, B. He, J. Sanati, Q. J. Wang, and T. J. Marks, *Chemistry of Materials*, 2008, 20, 5438-5443.
5. C. N. R. Rao and A. Nag, *European Journal of Inorganic Chemistry*, 2010, 2010, 4244-4250.
6. C. Lee, H. Yan, L. E. Brus, T. F. Heinz, J. Hone, and S. Ryu, *ACS Nano*, 2010, 4, 2695-2700.
7. N. Zeng, D. G. Hopkinson, B. F. Spencer, S. G. McAdams, A. A. Tedstone, S. J. Haigh, and D. J. Lewis, *Chemical Communications*, 2019, 55, 99-102.